# Unusual Ferromagnetic Couplings in Single End-to-End Azide-Bridged Cobalt(II) and Nickel(II) Chain Systems

**Chang Seop Hong,[a] Ja-eung Koo,[a] Sang-Kil Son,[b] Yoon Sup Lee,*[b] Yaung-Soo Kim,[c] and Youngkyu Do*[a]**

**Abstract:** Two new one-dimensional single azide-bridged metal(II) compounds $[\{M(5\text{-methylpyrazole})_4(N_3)\}_n](ClO_4)_n(H_2O)_n$ [M = Co (**1a**), Ni (**2a**)] were prepared by treating an $M^{II}$ ion with stoichiometric amount of sodium azide in the presence of four equivalents of the 3(5)-methylpyrazole ligand. The isostructural compounds **1a** and **2a** crystallize in the monoclinic space group $P2_1/n$. The azide bridging ligands have a unique end-to-end coordination mode that brings two neighboring metal centers into a *cis*-position with respect to the azide unit to form single end-to-end azide-bridged cobalt(II) and nickel(II) chains. The two neighboring metal atoms at inversion centers adopt octahedral environments with four equatorial 3(5)-methylpyrazole ligands and two axial azide bridges. Two adjacent equatorial least-squares planes form dihedral angles of 60.5° and 60.6° for Co and Ni, respectively. In addition, the metal-azide-metal units form large M-$N_3$-M torsion angles, which are magnetically important geometrical parameters, of 71.6° for M = Co and 75.7° for M = Ni. It should also be noted that the M-N-N angles associated with end-to-end azide group, another magnetically important structural parameter, fall into the experimentally observed range of 120–140° as 128.3(3) and 147.8(3)° for cobalt species and 128.4(2) and 146.1(3)° for nickel species; these values deviate from the theoretical value of around 164° at which the incidental orthogonality is achieved under the torsion angle of 0°. The compounds **1a** and **2a** have unique magnetic properties of ferromagnetism, zero-field splitting, and spin canting. The MO calculations indicate that the quasi-orthogonality between the magnetic orbitals of metal ions and the p atomic orbitals of the bridging azide is possible in the observed structures and leads to the ferromagnetism. The spin canting related to the perturbation of ferromagnetism arises from the magnetic anisotropy and antisymmetric interactions judged by the structural parameters of the zero-field splitting and the tilted $MN_4$ planes in a chain. The enhancement of magnetic interactions was accomplished by dehydrating the chain compounds to afford two soft magnets with critical temperature $T_C$ and coercive field of 2 K and 35 G for **1b** and 2.3 K and 20 G for **2b**, respectively.

**Keywords:** azide · cobalt · magnetic properties · nickel · spin canting

## Introduction

The field of molecular magnets has been actively investigated in the last two decades with the hope of its promising applications to the future technology.[1] Several different strategies are currently employed in order to develop molecule-based magnetic materials that exhibit spontaneous magnetization. The discovery of the charge-transfer complex $[Fe(Me_5Cp)_2][TCNE]$ ($Me_5Cp$ = pentamethylcyclopentadienyl, TCNE = tetracyanoethylene) with $T_C = 4.8$ K pushed magnetochemists toward every endeavor with the aim of synthesis and design of new molecular magnets.[2] Along this line, the nonmagnetic ligand-based bimetallic $Mn^{II}-Cu^{II}$ complex $[MnCu(pbaOH)]\cdot 2H_2O$ (pbaOH = 2-hydroxy-1,3-propylenebis(oxamate), $T_C = 30$ K)[3] and the radical ligand-based complex $[Mn(hfac)_2(NITR)]$ (hfac = hexafluoroacetylactonate, NITR = 2-R-4,4,5,5-tetramethyl-4,5-dihydro-1-*H*-imidazolyl-1-oxy-3-oxide, $T_C = 7.8$ K for R = isopropyl)[4] were characterized. In more recent years, cyanide-based assemblies similar to Prussian blue were reported for $Cs_2Mn[V(CN)_6]$ ($T_C$ = 125 K),[5] $Cs_{0.75}Cr_{1.125}[Cr(CN)_6]$ ($T_C = 190$ K),[6] $(Et_4N)_{0.5}Mn_{1.25}[V(CN)_5]\cdot 2H_2O$ ($T_C = 230$ K),[5] and $V[Cr(CN)_6]_{0.86}$ ($T_C$ = 315 K).[7] The cyanide-bridged iron–nickel and iron–

[a] Prof. Y. Do, C. S. Hong, J.-e. Koo
Department of Chemistry, School of Molecular Science-BK21
and Center for Molecular Design and Synthesis
Korea Advanced Institute of Science and Technology
Daejeon 305-701 (Korea)
Fax: (+82) 42-869-2810
E-mail: ykdo@kaist.ac.kr

[b] Prof. Y. S. Lee, S.-K. Son
Department of Chemistry, School of Molecular Science-BK21
Korea Advanced Institute of Science and Technology
Daejeon 305-701 (Korea)

[c] Dr. Y.-S. Kim
Korea Basic Science Institute
Daejeon 305-333 (Korea)

Supporting information for this article is available on the WWW under http://www.wiley-vch.de/home/chemistry/ or from the author.

  0947-6539/01/0719-4243 $ 17.50+.50/0 

manganese systems coupled ferrimagnetically were added to the field of magnetic materials.[8]

In the light of factors that affect magnetic exchange pathways between the paramagnetic centers, the proper use of bridging ligands is of importance, since they influence the magnetic strength and nature in a molecule. In this regard, the azide ligand has been employed because it has the merit of diverse binding modes that directly bring about the variation of magnetic properties according to its orientation with respect to the magnetic centers.[9] In fact, many azide complexes with a wide range of structural variety spanning from dinuclear,[10] tetranuclear,[11] cubane,[12] one-dimensional,[13] two-dimensional,[14] to three-dimensional[15] arrays have been reported to date. The bridging azide ligand binds in an end-on mode for ferromagnetic and end-to-end mode for antiferromagnetic coupling in general. In the case of the end-to-end mode, the azide system with ferromagnetic coupling lacks an example, even though theoretical consideration predicts the presence of such systems.[13] It is well known that the magnetic nature of compounds is substantially correlated with their molecular structures. In addition, tuning of the capping ligands bound to metal ions can vary the coordination sphere around the magnetic centers. Thus, it would be of interest to apply diverse binding motifs to azide systems in the search for hitherto unprecedented ferromagnetic end-to-end azide complexes.

Efforts to design new magnetic materials have been made in our group and have afforded the observations of novel high-dimensional metal complexes, including a two-dimensional ferrimagnetic bimetallic compound linked by a dicarboxylate ligand[16] and a three-dimensional manganese(II) network connected by a terephthalato bridge.[17] In the latter system, the necessity of tuning the capping ligand that fills up the coordination sphere has been observed, since the use of nonchelating capping ligands seems to have broad relevance to the construction of the solid-state architecture and crystal engineering, presumably due to its ability to allow the complexation process some freedom.[17] By taking the role of capping ligands into consideration, attempts to use a nonchelating capping ligand, 3(5)-methylpyrazole, have been made to attain new azide complex systems with interesting properties. Herein, we report the details of the syntheses, structures, and properties of new one-dimensional compounds $[\{M(5\text{-methylpyrazole})_4(N_3)\}_n](ClO_4)_n(H_2O)_n$ (M = Co (**1a**), Ni(**2a**)). Part of the results for the nickel compound has been recently communicated.[18] The chain compounds **1a** and **2a** constitute the first examples of single end-to-end azide-bridged ferromagnetic systems.[13] The dehydrated forms of **1a** and **2a**, labeled as **1b** and **2b**, respectively, have been also investigated to elucidate the effect of the loss of lattice water molecules in the solid state on the magnetic strength, accounts of which are also described in this report along with the result of the MO calculation on the role of the magnetic pathway through the azide bridge in **2a**.

## Results and Discussion

**Syntheses and characterization**: The preparation of $[\{Co(5\text{-methylpyrazole})_4(N_3)\}_n](ClO_4)_n(H_2O)_n$ (**1a**) is relatively straightforward since the formation of mononuclear compound $[Co(5\text{-methylpyrazole})_4(N_3)_2]$[19] was not encountered when a 1:4:1 stoichiometric ratio of $Co^{II}$/3(5)-methylpyrazole/$N_3$ was employed. On the other hand, the synthesis of $[\{Ni(5\text{-methylpyrazole})_4(N_3)\}_n](ClO_4)_n(H_2O)_n$ (**2a**) requires not only careful use of right stoichiometry of the reagents, but also slow addition of the aqueous solution of sodium azide to the aqueous reaction mixture of $Ni^{II}$ and 3(5)-methylpyrazole. The use of 1:2:2 and 1:4:2 stoichiometric ratios of $Ni^{II}$/3(5)-methylpyrazole/$N_3$ gave mononuclear species $[Ni(5\text{-methylpyrazole})_4(N_3)_2]$.[20] Even in the case of the use of 1:4:1 stoichiometry of $Ni^{II}$/3(5)-methylpyrazole/$N_3$, the formation of $[Ni(5\text{-methylpyrazole})_4(N_3)_2]$ as blue precipitate proceeded prior to the formation of **2a** unless the aqueous solution of sodium azide was added slowly to the aqueous reaction mixture of $Ni^{II}$ and 3(5)-methylpyrazole. Reasons for this may include the poor solubility of $[Ni(5\text{-methylpyrazole})_4(N_3)_2]$ relative to that of **2a** and the increased stability of $[Ni(5\text{-methylpyrazole})_4(N_3)_2]$ judged by the lack of reactivity with respect to its conversion to **2a** in the presence of a one-fold amount of $Ni^{II}$ and a four-fold 3(5)-methylpyrazole.

The IR spectrum of **1a** contains one sharp band at 2092 $cm^{-1}$ attributable to the stretching frequency of azide ligand. The lattice water molecule possesses two stretches at 3581 and 3347 $cm^{-1}$, the latter of which is overlapped with the $\nu$(NH) band of 3(5)-methylpyrazole ligand. These strong and broad bands are due to the existence of hydrogen bonds. The bending band of lattice water molecule is observed at 1608 $cm^{-1}$.[21] The IR spectrum of **2a** is similar to that of **1a**, indicating that they are isostructural.

Based on the crystal structures of **1a** and **2a** (vide infra), between the chains there are water molecules that are hydrogen bonded to neighboring oxygen and nitrogen atoms and mediate weak magnetic exchange couplings. Dehydration of these compounds was attempted to eliminate the lattice water molecules under $N_2$ flow with the aim of the amplification of interchain magnetic communications that would generate long-range ordering in the lattice. The IR spectra show that the stretching bands at 3581 $cm^{-1}$ for **1a** and at 3585 $cm^{-1}$ for **2a** disappear upon dehydration, while the bands at 3347 $cm^{-1}$ for **1a** and 3353 $cm^{-1}$ for **2a** still exist due to the presence of $\nu$(NH). In addition, the HOH bending absorptions at 1604 $cm^{-1}$ for **1a** and 1608 $cm^{-1}$ for **2a** also disappear upon heating, indicating complete loss of the water molecules in lattice.[21] The dehydrated samples **1b** and **2b** reabsorb water molecules from air and return to the hydrated forms; this was verified by IR spectroscopy and TGA measurements.

**Structures**: The crystal structures of $[\{M(5\text{-methylpyrazole})_4(N_3)\}_n](ClO_4)_n(H_2O)_n$ (M = Co, Ni) consist of one-dimensional $M^{II}$ chains with isolated perchlorate anions and lattice water molecules. Both species **1a** and **2a** are isostructural and their molecular views are nearly the same. A molecular view of the asymmetric unit and one symmetry-related fragment along with the atom labeling scheme for **1a** is taken as a representative illustration and is displayed in Figure 1 (top). Selected bond lengths and angles for both are given in



0947-6539/01/0719-4244 $ 17.50+.50/0 *Chem. Eur. J.* **2001**, *7*, No. 19

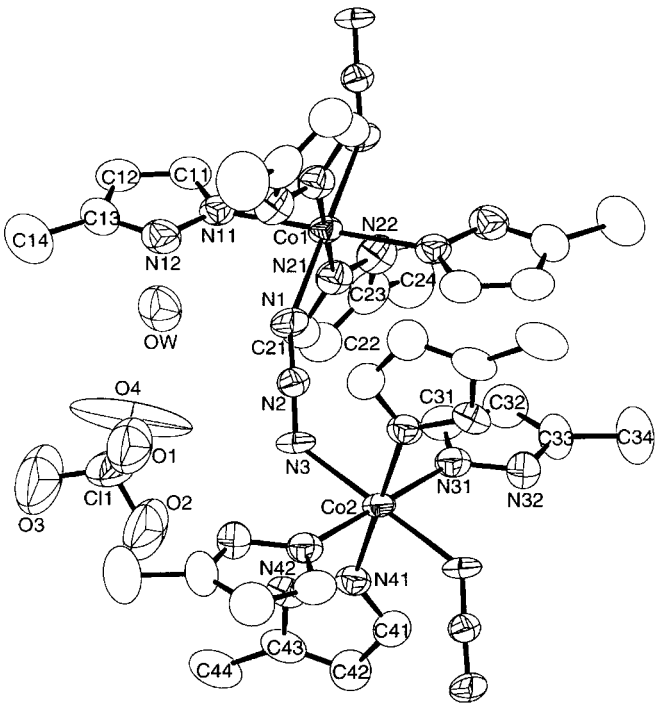


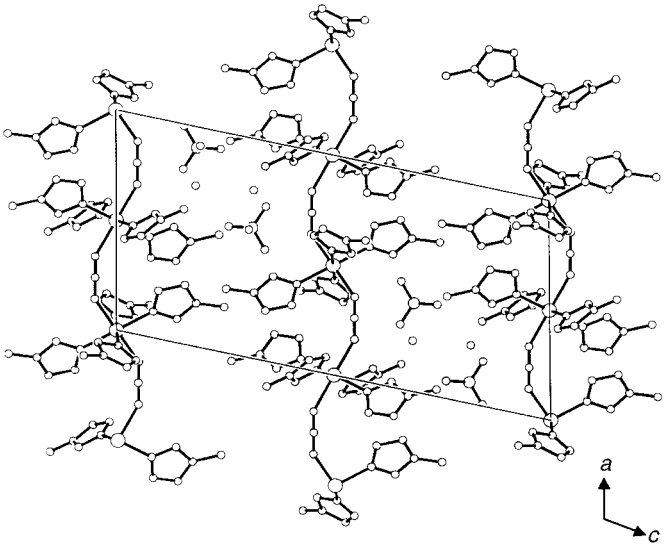


Figure 1. Top: Perspective view of the asymmetric unit along with the atom-labeling scheme and 50% thermal ellipsoids for **1a**. Bottom: View of **1a** in the *ac* plane.

Table 1. Perspective structural views of isostructural **2a** are deposited as Supporting Information.

The two metal atoms at inversion centers adopt octahedral environments. One metal center has relatively uniform bond lengths to the surrounding nitrogen atoms of the equatorial 3(5)-methylpyrazole ligands and axial azide bridges, while the other center has more distorted geometry that results from a slight equatorial contraction of the capping ligands and axial elongation of the azide bridges. Two equatorial least-squares planes that contain two adjacent M atoms associated with four

Table 1. Selected interatomic distances [Å] and angles [°] for **1a** and **2a**.

| **1a** | | **2a** | |
|---|---|---|---|
| Co1–N21 | 2.116(4) | Ni1–N1 | 2.124(3) |
| Co1–N11 | 2.139(4) | Ni1–N21 | 2.082(3) |
| Co1–N1 | 2.167(4) | Ni1–N11 | 2.097(3) |
| N1–N2 | 1.164(5) | N11–C11 | 1.328(4) |
| N2–N3 | 1.171(5) | N1–N2 | 1.158(4) |
| N3–Co2 | 2.141(4) | N2–N3 | 1.177(4) |
| Co2–N31 | 2.144(4) | N3–Ni2 | 2.098(3) |
| Co2–N41 | 2.145(4) | Ni2–N41 | 2.105(3) |
| Co1 ··· Co2 | 5.774 | Ni2–N31 | 2.106(3) |
| | | Ni1 ··· Ni2 | 5.715 |
| N21-Co1-N11 | 92.48(15) | N1-Ni1-N21 | 92.19(12) |
| N21-Co1-N1 | 87.50(15) | N21-Ni1-N21 | 180.0 |
| N11-Co1-N1 | 86.77(15) | N1-Ni1-N11 | 87.69(11) |
| N2-N1-Co1 | 147.8(3) | N21-Ni1-N11 | 87.22(12) |
| N1-N2-N3 | 178.7(4) | C11-N11-Ni1 | 129.6(2) |
| N2-N3-Co2 | 128.3(3) | N12-N11-Ni1 | 126.0(2) |
| C11-N11-Co1 | 129.4(3) | C21-N21-Ni1 | 131.1(3) |
| N12-N11-Co1 | 126.0(3) | N22-N21-Ni1 | 13.4(2) |
| C21-N21-Co1 | 131.0(3) | N2-N1-Ni1 | 146.1(3) |
| N22-N21-Co1 | 123.9(3) | N3-N2-N1 | 177.8(3) |
| N3-Co2-N31 | 91.6(2) | N2-N3-Ni2 | 128.4(2) |
| N3-Co2-N41 | 92.05(15) | N41-Ni2-N31 | 92.46(11) |
| N31-Co2-N41 | 92.14(14) | N41-Ni2-N3 | 92.08(12) |
| C31-N31-Co2 | 130.5(3) | N31-Ni2-N3 | 89.12(11) |
| N32-N31-Co2 | 124.6(3) | C31-N31-Ni2 | 130.6(3) |
| C41-N41-Co2 | 132.1(3) | N32-N31-Ni2 | 124.5(2) |
| N42-N41-Co2 | 122.8(3) | C41-N41-Ni2 | 131.8(3) |
| | | N42-N41-Ni2 | 122.9(2) |

equatorial nitrogen atoms of 3(5)-methylpyrazole ligands are not parallel and form dihedral angles of 60.5° and 60.6° for Co and Ni, respectively.

Another perspective view of **1a** in the *ac* plane shown in Figure 1 (bottom) demonstrates that the azide bridging ligands have a unique end-to-end coordination mode that brings two neighboring metal centers into a *cis*-position with respect to the azide unit to form single end-to-end azide-bridged cobalt(II) and nickel(II) chains. This marks the first examples, to our knowledge, of the single-chain $\mu$-azido cobalt(II) and nickel(II) system with end-to-end coordination of the $N_3$ group.[13] In addition, the metal-azide-metal unit forms a large M-$N_3$-M torsion angle, which is a magnetically important geometrical parameter,[13] of 71.6° for M = Co and 75.7° for M = Ni. Note that the difference between two values of torsion angles is relatively large for the isostructural species. Such a unique coordination mode and large torsion angle might be considered as a manifestation of the structural freedom of the nonchelating capping ligands in complexation process. It should also be noted that the M-N-N angles of the end-to-end azide group, another magnetically important structural parameter, fall into the experimentally observed range of 120–140° as 128.3(3) and 147.8(3)° for cobalt species and 128.4(2) and 146.1(3)° for nickel species; these values deviate from the theoretical value of around 164° at which the incidental orthogonality is achieved under the torsion angle of 0°.[13]

The intrachain distances between the adjacent metal ions are 5.774 and 5.717 Å, and the shortest interchain metal–metal distances are 9.807 and 9.815 Å for **1a** and **2a**, respectively. In both cases, the lattice water molecules are

hydrogen bonded to the perchlorate oxygen atoms and to the capping 3(5)-methylpyrazole ligand nitrogen atoms.

**Magnetic properties of hydrated species 1a and 2a**

*Ferromagnetic interactions*: The temperature dependence of the magnetic susceptibilities measured at 100 G is shown in Figure 2 in the range of 1.8–300 K. For **1a** (Figure 2, top), the $\chi_m T$ value at 300 K is equal to 3.17 $cm^3 K mol^{-1}$, which is

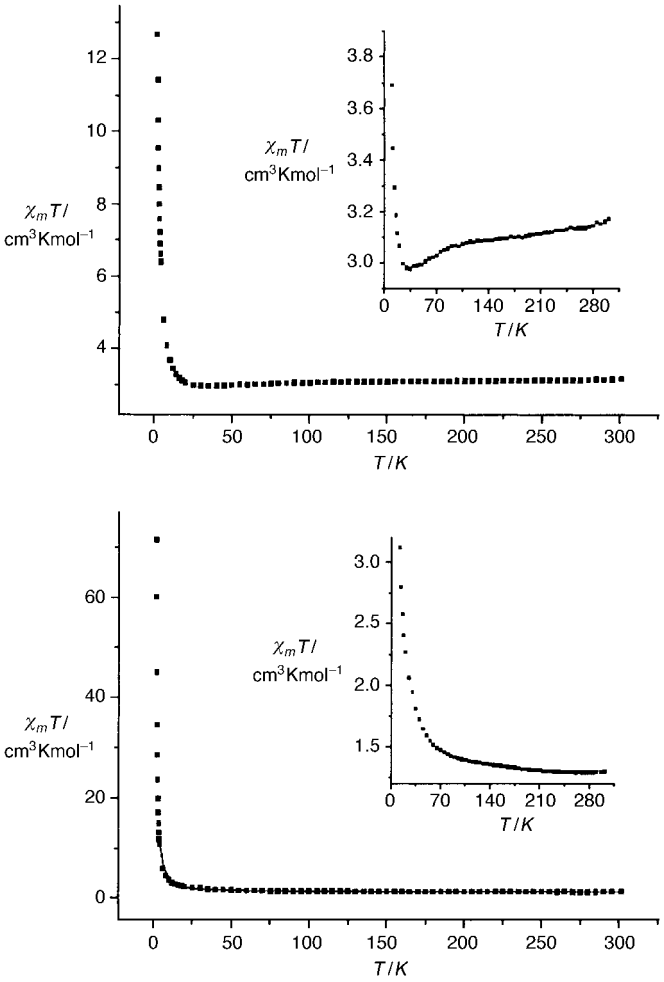


Figure 2. Plot of temperature dependence of the $\chi_m T$ of **1a** (top) and **2a** (bottom). The solid line for **2a** shows the best theoretical fit.

higher than the spin-only value (1.88 $cm^3 K mol^{-1}$) owing to unquenched orbital contribution of the high-spin octahedral $Co^{II}$ complex.[22] On lowering the temperature, the $\chi_m T$ value gradually decreases to a value of 2.98 $cm^3 K mol^{-1}$ at 35 K as a result of spin-orbit coupling effects,[23] and then abruptly increases to a value of 12.67 $cm^3 K mol^{-1}$ at 1.8 K; this is an indication of the presence of ferromagnetic exchange coupling in the chain. On the other hand, for complex **2a** (Figure 2, bottom), as the temperature decreases the $\chi_m T$ value of 1.30 $cm^3 K mol^{-1}$ at 300 K increases gradually to 4.38 $cm^3 K mol^{-1}$ at 8 K and then rises sharply to reach a value of 71.51 $cm^3 K mol^{-1}$ at 1.8 K; this is an indication of the onset of long-range interactions in the lattice.

Fitting the magnetic data to the Curie-Weiss law ($\chi_m = C/(T-\theta)$) gives a Weiss constant of $\theta = 2.44$ K with a Curie constant of $C = 2.74\ cm^3 K mol^{-1}$ ($g = 2.41$) for **1a** in the temperature range of 6–35 K, and $\theta = 11.1$ K with $C = 1.24\ cm^3 K mol^{-1}$ ($g = 2.23$) for **2a** in the temperature range of 30–300 K.[24] The positive Weiss constants indicate that there are ferromagnetic interactions between $M^{II}$ magnetic centers bridged by azide ligand with end-to-end coordination. The magnitude of the Weiss constant of **2a** is stronger than that of **1a**. This may be interpreted in terms of the shorter intrachain metal–metal distance (5.717 Å) for **2a** than that (5.774 Å) of **1a**, which causes stronger magnetic interactions, and the larger torsion angle (75.7°) of **2a** than that (71.6°) for **1a**, which mediates ferromagnetic couplings more effectively in terms of the incidental orthogonal point (vide infra). In the case of **2a**, the best fit with $S_A = 1$ of the observed magnetic data to an infinite chain model ($H = -J\Sigma S_{Ai} S_{Ai+1}$) expressed as Equation (1),[25] in the temperature range of 4–300 K, yields parameters of $g = 2.21$ and $J = 6.91\ cm^{-1}$. The theoretical result affords a satisfactory agreement with the experimental data points as illustrated in Figure 2 (bottom). The measure of the goodness of fit $R$, defined as $R = [\Phi/(n-k)]^{1/2}$, in which $n$ is the number of data points, $k$ is the number of parameters, and $\Phi = \Sigma[(\chi_m T)_i^{obs} - (\chi_m T)_i^{calcd}]^2$, is equal to $1.8 \times 10^{-3}$.

$$\chi_m = \{Ng^2\beta^2 S_A(S_A + 1)/3kT\}\{(1+u)/(1-u)\} \quad (1)$$

$$u = \coth[JS_A(S_A + 1)/kT] - [kT/JS_A(S_A + 1)] \quad (1a)$$

The positive $J$ value suggests the presence of a ferromagnetic exchange interaction transmitted by the azide group in the chain. It should be noted that the compounds **1a** and **2a** constitute the first ferromagnetic examples of singly bridged $\mu$-azido complexes with end-to-end coordination of $N_3$, since all azide compounds with the same bridging mode reported to date have antiferromagnetic ordering.[26]

*Orbital interpretation of the magnetic behavior*: According to the bibliographic data,[13] the magnetic properties of the azide complexes depend on M-N-N(azido) angles and M-$N_3$-M torsion angles, and the occurrence of a ferromagnetic coupling can be expected when the incidental orthogonality is achieved at the value of about 164° for M-N-N(azido) angle at fixed zero M-$N_3$-M torsion angle, while the strongest antiferromagnetic interaction is expected when the M-$N_3$-M torsion angle closes to zero for a fixed M-N-N(azide) angle. According to these criteria, the expected magnetic phenomena for **1a** and **2a** would be antiferromagnetic ordering, since their M-N-N-(azido) angles deviate far from 164°. This expectation is in conflict with the experimental results of ferromagnetic behavior. Therefore, the resolution of this conflict was attempted by considering the large M-$N_3$-M torsion angles of 71.6° and 75.7°; these may minimize antiferromagnetic contributions and favor ferromagnetic interactions in chains of **1a** and **2a**.[13]

To get a better insight into the magnetic exchange mechanism, extended Hückel calculations were performed on the dimeric fragment of **2a** with the use of the X-ray crystal coordinates. The magnetically active atomic orbitals of the



0947-6539/01/0719-4246 $ 17.50+.50/0 *Chem. Eur. J.* **2001**, *7*, No. 19

$Ni^{II}$ ions are the $d_{z^2}$ orbitals, since they are placed in the chain direction and provide symmetric ($\Phi_s$) and antisymmetric ($\Phi_a$) combinations (Figure 3). The magnetic orbitals of $Ni^{II}$ ions

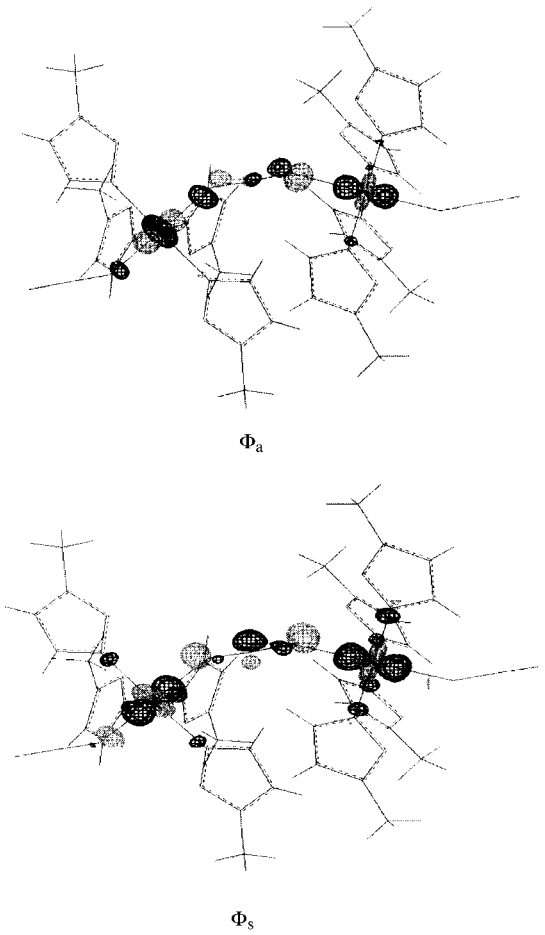


Figure 3. The MO representation of **2a** showing π pathway through the azide bridge.

overlap with p atomic orbitals of an azide bridging ligand in a π pathway, and the azide p orbitals are almost orthogonal as judged by the fact that the atomic orbital of N1 is placed in the same plane with that of N3, but perpendicular to that of N2. Since this quasi-orthogonality allows the minimal overlap integrals through the bridge, the antiferromagnetic contribution ($J_{ij}^{AF}$) to $J = (1/n^2)\Sigma_{ij}J_{ij}$,[27] the magnetic exchange coupling of systems with more than two unpaired electrons, in the magnetic regime may be negligible relative to the ferromagnetic one. Hence, it is plausible to conclude that a net ferromagnetic exchange coupling in the azide chain system of **2a** is favored, which is in good agreement with the magnetic consequence of **2a**.

*Zero-field splitting*: The plots of $\chi_m T$ versus $T$ as a function of the external field for both of the one-dimensional complexes are shown in Figure 4. There are no maximum points at low field, but the maximum points begin to appear and shift to high temperature as the field increases. These observations suggest that thermal populations of the Zeeman levels are located in the lowest level at lower fields and are mixed at

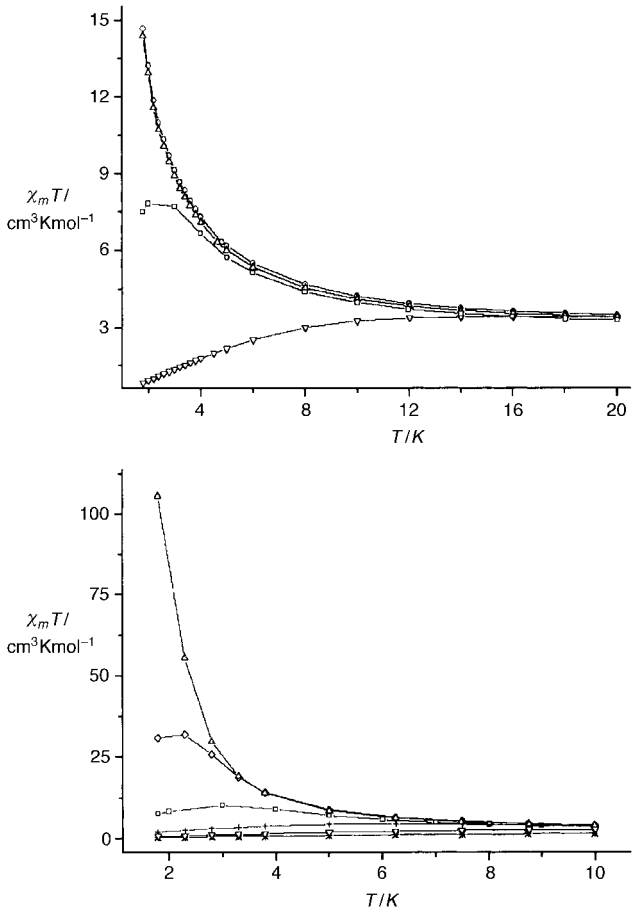


Figure 4. $\chi_m T$ versus T plots in the low-temperature range at various values of the applied field for **1a** (top) and **2a** (bottom). For **1a** the data were recorded at the following field strengths (top to bottom): 50, 100, 2000, 30000 G; for **2a** the data were recorded at the following field strengths (top to bottom): 100, 500, 2000, 10000, 30000, 70000 G. The solid lines joining the experimental points are just eye guides.

higher fields. Hence, the zero-field splittings in $M^{II}$ [M = Co (**1a**), Ni (**2a**)] ions are operative and cause the decrease in $\chi_m T$ at higher fields.

*Spin canting*: The magnetization $M$ of **1a** and **2a** were measured with variation of the applied magnetic field $H$ from 0 to 7 T at two temperatures of 1.8 and 5 K as given in Figure 5. The two complexes behave similarly since they are isostructural. The abrupt approaches of $M$ to the saturation values at 1.8 K are observed for both complexes; this behavior is reminiscent of magnets. No hysteresis loop is observed at 1.8 K in the field range from −7 to 7 T as shown in insets of Figure 5. The experimental saturation values at 7 T are 2.64 and 1.97 N$\beta$ for **1a** and **2a**, respectively. These values are slightly lower than the predicted values by the Brillouin equation [Eqs. (2)–(4)] with $S = 3/2$ (**1a**, $M \approx 3$ N$\beta$) and $S = 1$ (**2a**, $M \approx 2.2$ N$\beta$) at 1.8 K for noninteracting entities in a lattice.[28]

$$M = Ng\beta HSB_S(x) \quad (2)$$

$$B_S(x) = \{(2S + 1)/2S\}\coth[x(2S + 1)/2S] - \{1/2S\}\coth[x/2S] \quad (3)$$

$$x = g\beta HS/kT \quad (4)$$

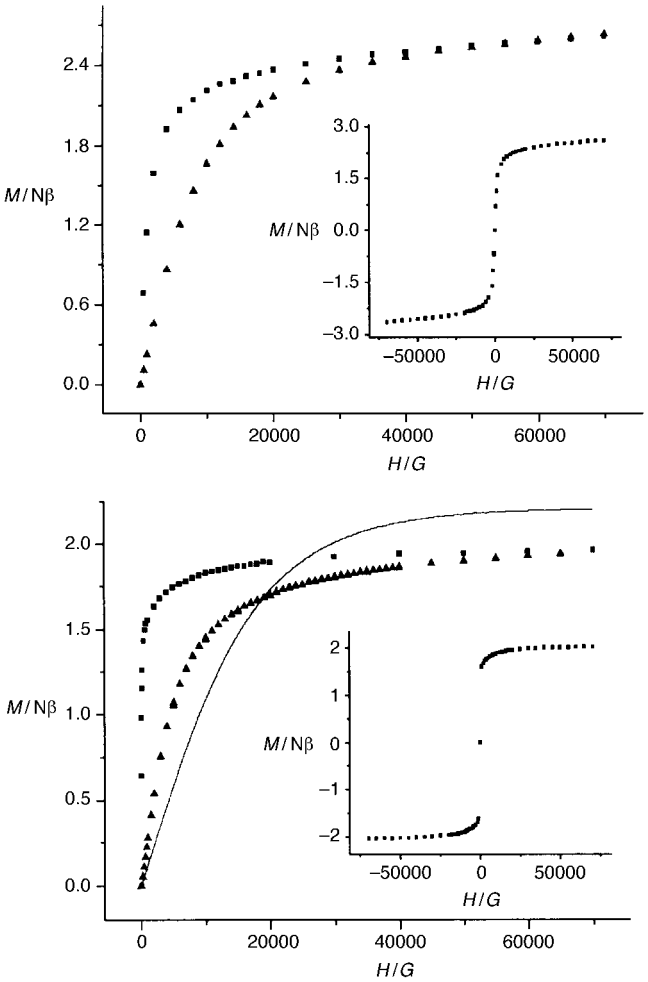


Figure 5. Plot of magnetization versus applied magnetic field for **1a** (top) and **2a** (bottom) at temperatures, 1.8 (■) and 5 K (▲). The solid line for **2a** represents the Brillouin calculation for $S=1$ state. The insets show hysteresis curves.

From this result, it appears that the spin values of the metal centers in the ground state are smaller than the expected values from the numbers of their unpaired electrons, hence spin canting is operative in both **1a** and **2a**. To take spin canting into account two factors need to be considered: the antisymmetric interaction and the magnetic anisotropy.[23] The least-squares planes that include the asymmetric $M^{II}$ units along the chain are tilted towards each other and form dihedral angles of 60.5° for **1a** and 60.6° for **2a**. This fulfills the requirement for the antisymmetric interaction. The magnetic anisotropy is intrinsic to the $Co^{II}$ or $Ni^{II}$ ion owing to the presence of zero-field splitting. In terms of the two factors, two possible patterns for spin canting can be suggested as illustrated in Figure 6. In Figure 6 (top), the directions of spin vectors for spin canting are oriented antiparallel, which results in a very low saturation magnetization; this is not in agreement with the experimental values. At the same time, the antiferromagnetic interaction gives rise to the feature that the $\chi_m T$ value decreases slowly to reach a round minimum and then increases rapidly at lower temperature.[29] However, the temperature dependence of the $\chi_m T$ value for **2a** does not follow the magnetic consequence predicted

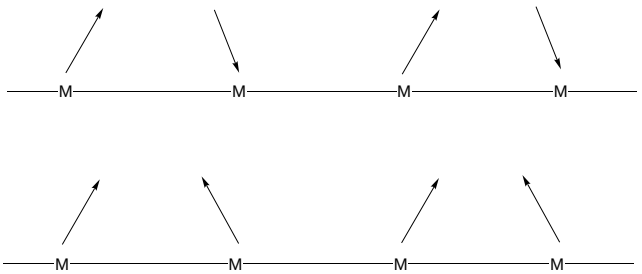


Figure 6. Schematic drawing of possible spin-canting patterns superimposing onto dominant antiferromagnetic interactions (top) and dominant ferromagnetic interactions (bottom).

by the spin-canting pattern shown in Figure 6 (top). On the other hand, Figure 6 (bottom) illustrates spin canting caused by the perturbation of ferromagnetism, that is, the magnetic spins are coupled ferromagnetically but are slightly tilted to each other. This pattern for spin canting gives relatively high values of saturation magnetization and requires no minimum valley in $\chi_m T$ curve as observed in **2a**.[30] The spin canting based on ferromagnetic coupling supports the experimental results well, in agreement with the expectation from the large torsion angles greater than 70° (vide supra). The canting angles are estimated as 28° and 27° for **1a** and **2a**, respectively.

*Field-cooled magnetization*: To establish a magnetic phase transition, magnetization measurements under a weak applied field of 3 G were performed at various temperatures. The magnetization curve, recorded by cooling the sample from 20 to 1.8 K, rapidly increases below about 3 K, as shown in Figure 7. The slope of $dM/dT$ in the magnetization plot increases even at the lowest experimental temperature limit of 1.8 K; this is an indication that the critical temperature ($T_C$) is lower than 1.8 K, but near to 1.8 K judged by the field dependence at 1.8 K as described above in Figure 5. The ac susceptibility was measured for **2a**; this method provides a more accurate $T_C$ by showing a maximum at the critical temperature. The real part of the zero-field ac susceptibility has no maximum at 1.8 K for a frequency of 5000 Hz, confirming that the $T_C$ of **2a** is lower than 1.8 K.

### Magnetic properties of dehydrated species 1b and 2b

*Enhanced magnetic interactions*: The magnetic properties of the dehydrated compounds were measured to evaluate the influence on the bulk magnetic character when the interchain distances were reduced by eliminating the lattice water molecules.[31] Temperature-dependent magnetic susceptibility data at 100 G for **1b** and **2b** are shown in Figure 8. The $\chi_m T$ values of both dehydrated species are enhanced relative to their hydrated complexes at the same magnetic field in the low temperature regime; this indicates that the interchain distances of the ferromagnetic chains are reduced upon the dehydration and the ferromagnetic chains are also coupled ferromagnetically.

The magnetic behavior of **1b** is similar to its hydrated form, while **2b** shows different behavior from its hydrated form. For **1b**, the $\chi_m T$ value gradually decreases due to the spin-orbit



0947-6539/01/0719-4248 $ 17.50+.50/0 *Chem. Eur. J.* **2001**, *7*, No. 19

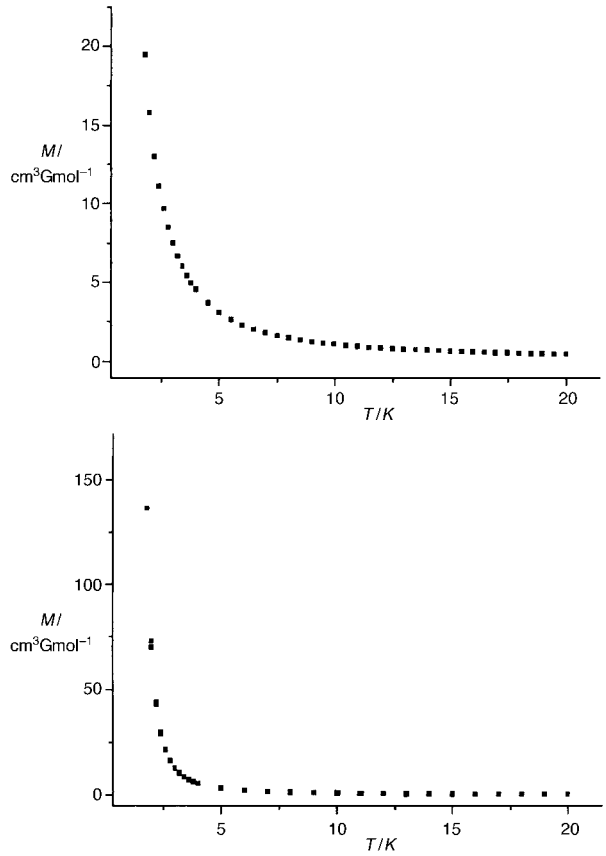


Figure 7. Field-cooled magnetization versus $T$ under 3G for **1a** (top) and **2a** (bottom).

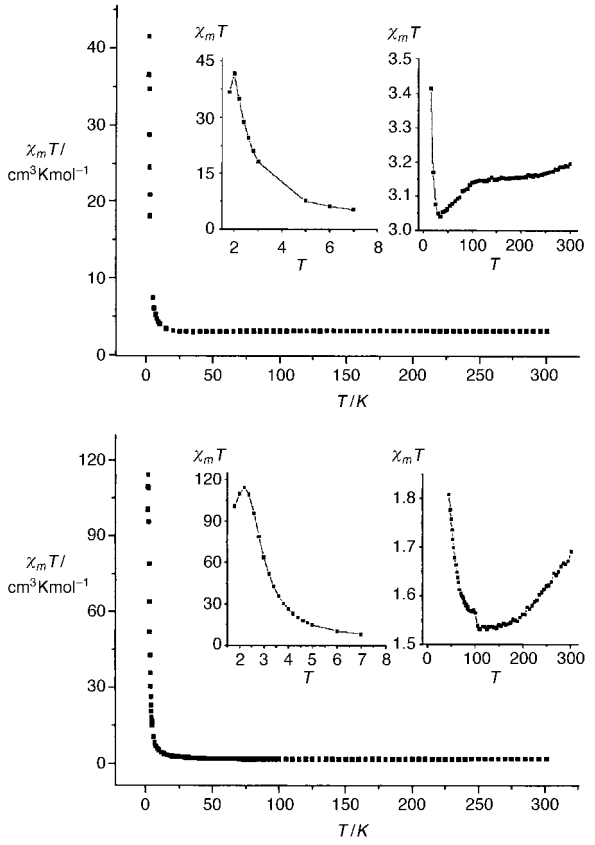


Figure 8. Plot of temperature dependence of the $\chi_m T$ for **1b** (top) and **2b** (bottom). The solid lines in insets are just eye guides.

coupling effects as temperature is lowered, reaches a minimum value of 3.04 $cm^3 K mol^{-1}$ at 35 K, then increases sharply as temperature decreases further to reach a maximum value of 41.54 $cm^3 K mol^{-1}$ at 2 K, and starts to decrease below 2 K due to the saturation effect. The $\chi_m T$ value of **2b** decreases slowly on lowering the temperature, increases rapidly below 9 K to reach a maximum value of 114.3 $cm^3 K mol^{-1}$ at 2.2 K, and then decreases owing to the saturation effect. The decrease of $\chi_m T$ value in the temperature range 300–9 K for **2b** can be considered to be a consequence of the spin-orbit coupling effects of the $Ni^{II}$ atoms triggered by additional structural change, presumably in Ni-$N_3$-Ni torsion angle, upon dehydration.

*Long-range ordering*: The long-range magnetic phase transitions for **1b** and **2b** were ascertained by the field-cooled magnetization (FCM) and the zero-field-cooled magnetization (ZFCM) measurements (Figure 9), which were recorded

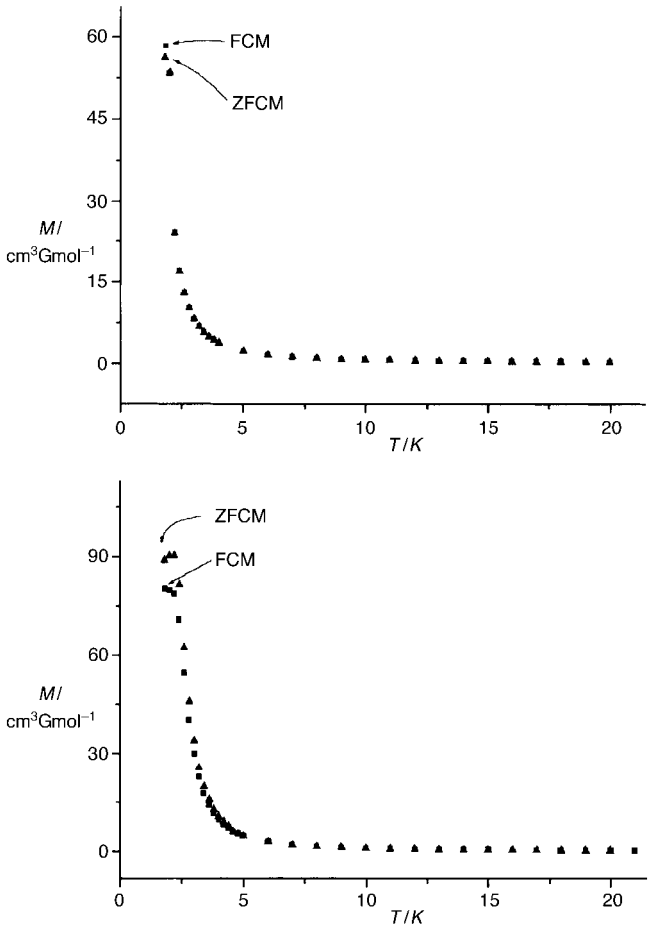


Figure 9. Plots of field-cooled magnetization (▲ FCM) and zero-field-cooled magnetization (■ ZFCM) in a field of 3 G for **1b** (top) and **2b** (bottom).

by cooling the sample down to 1.8 K under 3 G and warming up to 20 K in the same field and by cooling down without the applied field and then heating up in a field of 3 G, respectively. The FCM and ZFCM data indicate the occurrence of the phase transition near 2 K for **1b** and below 2.6 K for **2b**. The

accurate temperatures of the ferromagnetic phase transition were determined by measuring the thermal dependence of the in-phase ($\chi_m'$) and the out-of-phase ($\chi_m''$) components of the ac magnetic susceptibility (Figure 10). The $\chi_m'$ curve for **1b** shows frequency-independent curvatures at 2 K, taken as the critical temperature ($T_C$), which agrees with the appearance of non-zero $\chi_m''$ components. The $\chi_m'$ curve for **2b** has a maximum at $T_C = 2.3$ K at various frequencies with non-zero imaginary part, $\chi_m''$. These results denote that a disorder in the lattice, for example, spin-glass or superparamagnetic phenomena, is absent in **1b** or **2b**.

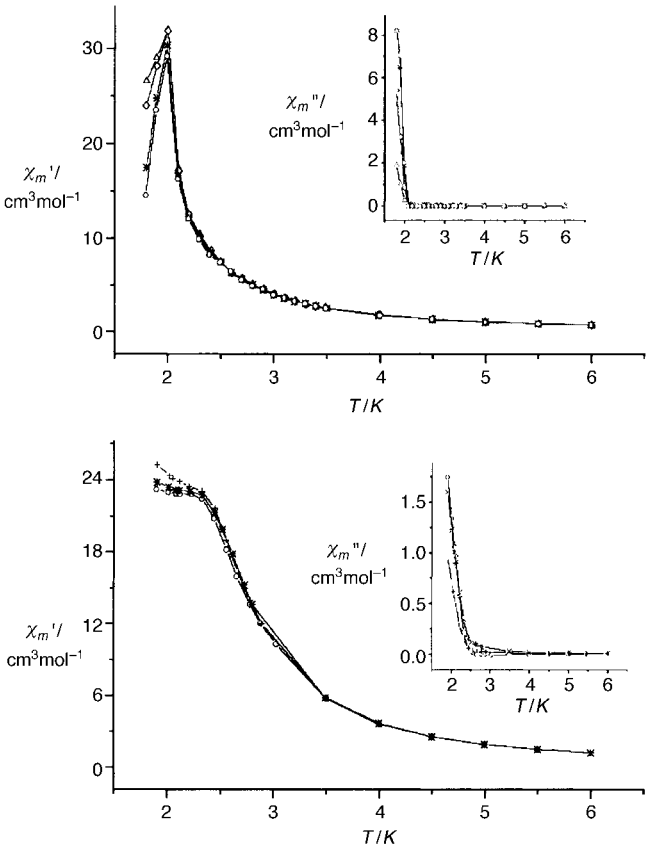


Figure 10. Real $\chi_m'$ and imaginary $\chi_m''$ parts of ac susceptibilities as a function of temperature at a dc field of ~0 G and an ac field of 3 G for **1b** (top) and **2b** (bottom). Frequencies for **1b** (from top to bottom): 100, 1000, 5000, 10000 Hz; frequencies for **2b** (from top to bottom): 500, 5000, 10000 Hz.

The magnetization measurements of **1b** and **2b** were performed as a function of field at various temperatures, as shown in Figure 11. The isotherms of **1b** exhibit typical ferromagnetic behavior and saturate faster than the hydrated complex **1a**. On the other hand, the shape of the magnetization of **2b**, which is similar to but much steeper than that of the hydrated species **2a**, is viewed as a real magnet at 1.8 K. The saturation values of 2.53 and 1.92 N$\beta$ at 7 T for **1b** and **2b**, respectively, imply that the magnetic spins on $M^{II}$ centers (M = Co, Ni) in a chain are ferromagnetically coupled but canted slightly. The magnetic hysteresis loops in the insets of Figure 11 are characteristic of soft magnets with a coercive field of 35 and 20 G for **1b** and **2b**, respectively.

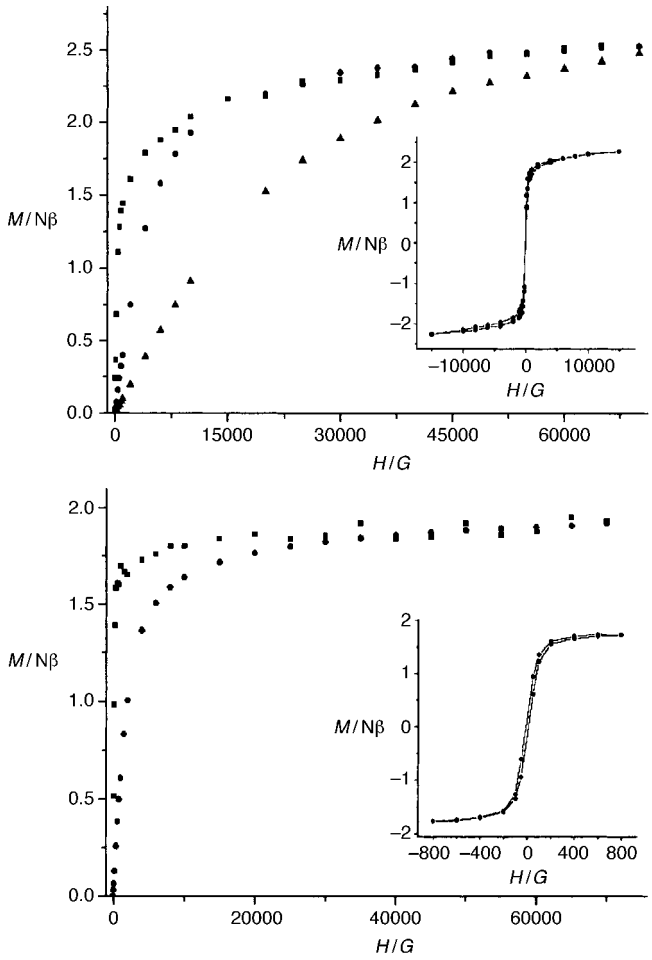


Figure 11. Plot of magnetization ($M$) versus applied magnetic field ($H$) for **1b** (top) and for **2b** (bottom), at various temperatures (■ 1.8 K, ● 5 K, ▲ 10 K). The insets show hysteresis curves.

## Conclusion

The first examples of the ferromagnetic $\mu$-azido one-dimensional single-chain systems with an end-to-end $N_3$ coordination mode, $[\{M(5\text{-methylpyrazole})_4(N_3)\}_n](ClO_4)_n(H_2O)_n$ [M = Co (**1a**), Ni (**2a**)], have been synthesized and characterized. For the synthesis of **2a**, the importance of the use of not only correct stoichiometry for the reagents, but also slow addition of the aqueous solution of sodium azide to the aqueous reaction mixture of $Ni^{II}$ and 3(5)-methylpyrazole has been pointed out to avoid the formation of paramagnetic mononuclear complex $[Ni(5\text{-methylpyrazole})_4(N_3)_2]$.

The magnetic susceptibility data for **1a** and **2a** in the temperature range of 1.8–300 K were interpreted by Curie–Weiss law and afforded the magnetic parameters of $\theta = 2.44$ K and $C = 2.74\ cm^3 K mol^{-1}$ for **1a**, and $\theta = 11.1$ K and $C = 1.24\ cm^3 K mol^{-1}$ for **2a**. The magnetic data of **2a** were also interpreted in terms of the infinite chain model with $J$ and $g$ values of 6.91 $cm^{-1}$ and 2.21, respectively; these values are consistent with the results from Curie–Weiss law. The occurrence of the abrupt increase in the $\chi_m T$ curve indicates the onset of a long-range ordering over the lattice. The compounds **1a** and **2a** acquire their ferromagnetism through



0947-6539/01/0719-4250 $ 17.50+.50/0 *Chem. Eur. J.* **2001**, *7*, No. 19

the quasi-orthogonality between the magnetic orbitals of metal ions and the p atomic orbitals of the bridging azide. Both compounds show spin canting caused by perturbation of ferromagnetism and zero-field splitting. The spin canting arises from the magnetic anisotropy and antisymmetric interactions judged by the structural parameters of zero-field splitting and the tilted $MN_4$ planes in a chain. The critical temperatures for **1a** and **2a** were not detected even at the temperature as low as 1.8 K. The observation that the $Ni^{II}$ compound exhibits stronger ferromagnetic strength than the $Co^{II}$ compound was explained in terms of the shorter intrachain $M\cdots M$ distance and the larger torsion angle of M-$N_3$-M and their relation to the effectiveness of magnetic exchange.

The dehydrated forms of **1a** and **2a** show enhanced ferromagnetic couplings due to the reduction of interchain distances of the chain systems as well as the ferromagnetic interactions between the chains. There is long-range magnetic ordering over the lattice as indicated by the critical temperatures of $T_C = 2$ K for **1b** and 2.3 K for **2b** determined from the magnetization at low temperatures and ac magnetic susceptibility experiments.

The use of a nonchelating capping ligand 3(5)-methylpyrazole in new azide systems led to the observation of the unprecedented examples of a ferromagnetic azide system with end-to-end $N_3$ coordination involving spin canting. It appears that the structural freedom of a capping ligand in the complexation plays a crucial role in generating a new class of single-chain ferromagnetic azide systems.

## Experimental Section

**Caution!** Azide and perchlorate systems are potentially explosive. The use of small amount of the reagents is recommended.

**[{Co(5-methylpyrazole)$_4$(N$_3$)}$_n$](ClO$_4$)$_n$(H$_2$O)$_n$ (1a)**: 3(5)-Methylpyrazole (160 μL, 2.0 mmol) was added to a solution of cobalt(II) perchlorate hexahydrate (182 mg, 0.50 mmol) in waater (10 mL). After being stirred for 10 min, a solution of sodium azide (32 mg, 0.50 mmol) in water (10 mL) was added. The red-brown solution was filtered, and the filtrate was left undisturbed, producing red-orange crystals of **1a** in a yield of 57%. Elemental analysis calcd (%) for $C_{16}H_{26}N_{11}O_5ClCo$ (546.86): C 35.14, H 4.79, N 28.17; found: C 35.17, H 4.79, N 28.61; IR (KBr pellet): $\tilde{\nu} = 3581$ (m), 3497 (w), 3448 (w), 3347 (s, NH stretching), 3149 (w), 2984 (w), 2932 (w), 2867 (w), 2092 (s, $\nu_a(N_3^-)$), 1754 (w), 1604 (w, HOH bending), 1569 (m), 1487 (w), 1445 (w), 1427 (w), 1346 (w), 1302 (w), 1111 (s, Cl-O stretching), 1017 (m), 952 (m), 881 (w), 804 (m), 788 (m), 726 (w), 691 (w), 623 (m), 420 cm$^{-1}$ (w).

**[{Ni(5-methylpyrazole)$_4$(N$_3$)}$_n$](ClO$_4$)$_n$(H$_2$O)$_n$ (2a)**: Compound **2a** was prepared by using the same procedure described for compound **1a**, but with nickel(II) perchlorate hexahydrate instead of the cobalt(II) salt and slow addition of azide solution in dropwise manner. The pale green solution was filtered, and the filtrate was left undisturbed, affording blue crystals of **2a** (36% yield). Elemental analysis calcd (%) for $C_{16}H_{26}N_{11}O_5ClNi$ (546.64): C 35.16, H 4.79, N 28.19; found: C 35.15, H 4.94, N 28.56; IR (KBr pellet): $\tilde{\nu} = 3580$ (m), 3497 (m), 3449 (m), 3334 (s, NH stretching), 3151 (m), 2985 (w), 2931 (w), 2871 (w), 2090 (s, $\nu_a(N_3^-)$), 1989 (w), 1763 (w), 1608 (w, HOH bending), 1573 (m), 1496 (m), 1447 (m), 1419 (m), 1349 (w), 1295 (m), 1225 (w), 1102 (s, broad, Cl-O stretching), 1018 (m), 952 (s), 885 (m), 803 (s), 785 (s), 689 (m), 623 (m), 425 cm$^{-1}$ (w).

**Dehydrated Compounds 1b and 2b**: Thermogravimetric analysis for **1a** and **2a** was carried out in the temperature range of 30–400 °C with a heating rate of 5 °C min$^{-1}$. The loss of lattice water was completed below 94 °C for **1a** and below 70 °C for **2a**. Thus, the dehydration was carried out by heating the samples to the proper temperatures for 5 h under the $N_2$ flow, and the resulting samples were dried overnight over a $P_2O_5$ trap in vacuum, to produce dehydrated products of cobalt-violet **1b** and pale blue **2b**. The asymmetric azide stretching frequency $\nu_a(N_3^-)$ in the IR spectra (Nujol mull) appeared at 2078 cm$^{-1}$ for **1b** and 2080 cm$^{-1}$ for **2b**.

**Physical measurements**: Elemental analyses for C, H, and N were performed at the Elemental Analysis Service Center of the Korea Basic Science Institute. Infrared spectra were recorded from KBr pellets with an EQUINOX 55 spectrometer. Thermal analyses were performed under the nitrogen atmosphere at a heating rate of 5 °C min$^{-1}$ with DuPont TA instruments. Measurement of magnetic susceptibilities, field dependencies of the magnetization, FCM, and ZFCM were carried out with a Quantum Design MPMS-7 SQUID magnetometer. The ac magnetic susceptibilities were determined above 1.8 K with a Quantum Design PPMS-9 magnetometer. Corrections for the diamagnetism of samples were estimated from Pascal's Tables.[32]

**Crystallographic data collection and structure determination**: Diffraction data for **1a** and **2a** were collected on an Enraf-Nonius CAD4TSB diffractometer by using graphite monochromated $Mo_{K\alpha}$ radiation ($\lambda = 0.71073$ Å). The unit cell parameters were calculated by least-squares refinement of 25 well-centered reflections in the range of $22.6° < 2\theta < 27.8°$ and $22.9° < 2\theta < 28.1°$ for **1a** and **2a**, respectively. Intensities of three reflections monitored periodically exhibited no significant variation for all cases. All data were corrected for Lorentz polarization effects. Crystal data and details of data collection are listed in Table 2.

Table 2. Crystallographic data for **1a** and **2a**.

| | **1a** | **2a** |
|---|---|---|
| formula | $C_{16}H_{26}N_{11}O_5ClCo$ | $C_{16}H_{26}N_{11}O_5ClNi$ |
| $M_r$ | 546.86 | 546.64 |
| crystal system | monoclinic | monoclinic |
| space group | $P2_1/n$ | $P2_1/n$ |
| $a$ [Å] | 11.548(9) | 11.434(1) |
| $b$ [Å] | 9.807(4) | 9.815(1) |
| $c$ [Å] | 22.677(20) | 22.576(1) |
| $\beta$ [°] | 102.40(7) | 102.68(1) |
| $V$ [Å$^3$] | 2508.3(31) | 2471.8(3) |
| $Z$ | 4 | 4 |
| $F(000)$ | 1132 | 1136 |
| $\rho_{calcd}$ [g cm$^{-3}$] | 1.448 | 1.469 |
| $\mu$ [mm$^{-1}$] | 0.840 | 0.943 |
| scan mode | $\omega$-$\theta$ | $\omega$-$2\theta$ |
| $2\theta$ range [°] | 4.4–50.02 | 4.4–49.94 |
| index range | $+h, +k, \pm l$ | $+h, +k, \pm l$ |
| reflections collected | 3827 | 3985 |
| reflections observed[a] | 2845 | 3390 |
| parameters | 310 | 310 |
| $R1$[b] | 0.0525 | 0.0482 |
| $wR2$[c] | 0.1343 | 0.1329 |
| weighting scheme[c] ($x/y$) | 0.0748/3.089 | 0.0759/2.656 |
| $\rho_{max}/\rho_{min}$ [e Å$^{-3}$] | 0.696/−0.352 | 0.578/−0.378 |

[a] $F_o > 4\sigma(F_o)$. [b] $R1 = \Sigma||F_o| - |F_c||/\Sigma|F_c|$. [c] $wR2 = [\Sigma\{w(F_o^2 - F_c^2)^2\}/\Sigma[w(F_o^2)^2]]^{1/2}$, in which $w = 1/[\sigma^2(F_o^2) + (xP)^2 + yP]$, $P = (F_o^2 + 2F_c^2)/3$.

The crystal structures were solved by direct methods by using the SIR92 program[33] and refined anisotropically for non-hydrogen atoms by full-matrix least-squares methods with the SHELXL93 program.[34] All hydrogen atoms were computed at ideal positions ($d_{CH} = 0.960$ Å for methyl and 0.930 Å for phenyl), except for hydrogens bound to water molecules, and refined riding on the corresponding carbon atoms with isotropic thermal parameters [$U = 1.5U(C_{methyl})$ and $1.2U(C_{phenyl})$]. The goodness of fit for all observed reflections was 1.121 for **1a** and 1.104 for **2a**. Maximum shift/e.s.d. were 0.021 (**1a**) and 0.000 (**2a**).

Crystallographic data (excluding structure factors) for the structures reported in this paper have been deposited with the Cambridge Crystallographic Data Centre as supplementary publication no. CCDC-162788 (**1a**) and CCDC-101870 (**2a**). Copies of the data can be obtained free of charge on application to CCDC, 12 Union Road, Cambridge CB2 1EZ, UK (fax: (+44) 1223-336-033; e-mail: deposit@ccdc.cam.ac.uk).

## Acknowledgements

This research was supported by the Korea Science and Engineering Foundation and the Korea Research Foundation in the program year 1997.

[1] a) C. P. Landee, M. Melville, J. S. Miller, *Magnetic Molecular Materials* (Eds.: D. Gatteschi, O. Kahn, J. S. Miller, F. Palacio), Kluwer, Dordrecht, **1991**, p. 395; b) O. Kahn, *Magnetism: A Supramolecular Function*, Kluwer, Dordrecht, **1996**; c) M. M. Turnbull, T. Sugimoto, L. K. Thompson, *Molecule-Based Magnetic Materials*, American Chemical Society, Washington DC, **1996**; d) J. S. Miller, A. J. Epstein, *Chem. Eng. News* **1995**, *73(40)*, 30.

[2] J. S. Miller, A. J. Epstein, W. M. Reiff, *Chem. Rev.* **1988**, *88*, 201.

[3] O. Kahn, Y. Pei, M. Verdaguer, J. P. Renard, J. Sletten, *J. Am. Chem. Soc.* **1988**, *110*, 782.

[4] a) A. Caneschi, D. Gatteschi, J. P. Renard, P. Rey, R. Sessoli, *Inorg. Chem.* **1989**, *28*, 1976; b) A. Caneschi, D. Gatteschi, J. P. Renard, P. Rey, R. Sessoli, *Inorg. Chem.* **1989**, *28*, 3314.

[5] W. R. Entley, G. S. Girolami, *Science* **1995**, *268*, 397.

[6] T. Mallah, S. Thienaut, M. Verdaguer, P. Veillet, *Science* **1993**, *262*, 1554.

[7] S. Ferlay, T. Mallah, R. Ouahès, P. Veillet, M. Verdaguer, *Nature* **1995**, *378*, 701.

[8] a) M. Ohba, H. Okawa, N. Fukita, Y. Hashimoto, *J. Am. Chem. Soc.* **1997**, *119*, 1011; b) H. Miyasaka, N. Matsumoto, H. Okawa, N. Re, E. Gallo, C. Floriani, *J. Am. Chem. Soc.* **1996**, *118*, 981.

[9] J. Ribas, M. Monfort, I. Resino, X. Solans, P. Rabu, F. Maingot, M. Drillon, *Angew. Chem.* **1996**, *108*, 2671; *Angew. Chem. Int. Ed. Engl.* **1996**, *35*, 2520.

[10] J. Ribas, M. Monfort, C. Diaz, C. Bastos, X. Solans, *Inorg. Chem.* **1993**, *32*, 3557.

[11] J. Ribas, M. Monfort, R. Costa, X. Solans, *Inorg. Chem.* **1993**, *32*, 695.

[12] M. A. Halcrow, J. C. Huffman, G. Christou, *Angew. Chem.* **1995**, *107*, 971; *Angew. Chem. Int. Ed. Engl.* **1995**, *34*, 889.

[13] a) A. Escuer, R. Vicente, J. Ribas, M. S. El Fallah, X. Solans, *Inorg. Chem.* **1993**, *32*, 1033; b) J. Ribas, M. Monfort, C. Diaz, C. Bastos, X. Solans, *Inorg. Chem.* **1994**, *33*, 484; c) A. Escuer, R. Vicente, J. Ribas, M. S. El Fallah, X. Solans, M. Font-Bardía, *Inorg. Chem.* **1994**, *33*, 1842; d) R. Vicente, A. Escuer, J. Ribas, M. S. El Fallah, X. Solans, M. Font-Bardía, *Inorg. Chem.* **1995**, *34*, 1278; e) J. Ribas, M. Monfort, B. K. Ghosh, R. Cortés, X. Solans, M. Font-Bardía, *Inorg. Chem.* **1996**, *35*, 864; f) M. A. Aebersold, B. Gillon, O. Plantevin, L. Pardi, O. Kahn, P. Bergerat, I. von Seggern, F. Tuczek, L. Öhrström, A. Grand, E. Lilièvre-Berna, *J. Am. Chem. Soc.* **1998**, *120*, 5238.

[14] M. Monfort, J. Ribas, X. Solans, *J. Chem. Soc. Chem. Commun.* **1993**, 350.

[15] F. A. Mautner, R. Cortés, L. Lezama, T. Rojo, *Angew. Chem.* **1996**, *108*, 96; *Angew. Chem. Int. Ed. Engl.* **1996**, *35*, 78.

[16] J. Kim, J. M. Lim, Y.-K. Choi, Y. Do, *Angew. Chem.* **1996**, *108*, 1079; *Angew. Chem. Int. Ed. Engl.* **1996**, *35*, 998.

[17] C. S. Hong, Y. Do, *Inorg. Chem.* **1997**, *36*, 5684.

[18] C. S. Hong, Y. Do, *Angew. Chem.* **1999**, *111*, 153; *Angew. Chem. Int. Ed.* **1999**, *38*, 193.

[19] The mononuclear complex $[Co(5\text{-methylpyrazole})_4(N_3)_2]$ was synthesized by the reaction of cobalt(II) perchlorate hexahydrate, 3(5)-methylpyrazole, and sodium azide in 1:4:2 molar ratio in aqueous solution. The yield was about 70% based on Co. Elemental analysis calcd (%) for $C_{16}H_{24}N_{14}Co$: C 40.77, H 5.13, N 41.60; found: C 40.58, H 5.21, N 42.12; crystal data ($Mo_{K\alpha}$, 293(2) K): monoclinic, $P2_1/c$, $a = 8.991(6)$, $b = 9.081(2)$, $c = 14.330(5)$ Å, $\beta = 107.75(3)^\circ$, $V = 1114.4(9)$ Å$^3$, $Z = 4$, blue-violet block, GOF = 1.140, $R = 4.03\%$ for 1362 observed independent reflections ($4.4^\circ < 2\theta < 48^\circ$); IR (KBr pellet): $\tilde{\nu} = 3305$ (s, NH stretching), 2077, 2061 cm$^{-1}$ (vs, $\nu_a(N_3^-)$).

[20] The mononuclear complex $[Ni(5\text{-methylpyrazole})_4(N_3)_2]$ was prepared by mixing the aqueous solution of nickel(II) perchlorate hexahydrate or nickel(II) acetate tetrahydrate with 3(5)-methylpyrazole and sodium azide in 1:4:2 molar ratio. The yield was ~80% based on Ni. Elemental analysis calcd (%) for $C_{16}H_{24}N_{14}Ni$: C 40.79, H 5.13, N 41.62; found: C 40.67, H5.18, N 42.03; crystal data ($Mo_{K\alpha}$, 293(2) K): monoclinic, $P2_1/c$, $a = 9.034(2)$, $b = 9.094(1)$, $c = 14.314(3)$ Å, $\beta = 107.95(2)^\circ$, $V = 1118.7(3)$ Å$^3$, $Z = 4$, blue block, GOF = 1.130, $R = 6.27\%$ for 1772 observed independent reflections ($4.4^\circ < 2\theta < 50^\circ$); IR (KBr pellet): $\tilde{\nu} = 3296$ (s, NH stretching), 2073, 2058 cm$^{-1}$ (vs, $\nu_a(N_3^-)$).

[21] K. Nakamoto, *Infrared and Raman Spectra of Inorganic and Coordination Compounds. Part B: Application in Coordination, Orgnometallic, and Bioinorganic Chemistry*, 5th ed., Wiley, New York, **1997**, p. 53.

[22] G. De Munno, M. Julve, F. Lloret, J. Faus, A. Caneschi, *J. Chem. Soc. Dalton Trans.* **1994**, 1175.

[23] F. Lloret, G. De Munno, M. Julve, J. Cano, R. Ruiz, A. Caneschi, *Angew. Chem.* **1998**, *110*, 143; *Angew. Chem. Int. Ed.* **1998**, *37*, 135.

[24] K. Nakayama, T. Ishida, R. Takayama, O. Hashizume, M. Yasui, F. Iwasaki, T. Nogami, *Chem. Lett.* **1998**, 497.

[25] C. Dupas, J.-P. Renard, *J. Chem. Phys.* **1974**, *61*, 3871.

[26] a) C. G. Pierpont, D. N. Hendrickson, D. M. Duggan, F. Wagner, E. K. Barefield, *Inorg. Chem.* **1975**, *14*, 604; b) A. K. Gregson, N. T. Moxon, *Inorg. Chem.* **1982**, *21*, 586; c) A. Escuer, R. Vincente, J. Ribas, M. S. El Fallah, X. Solans, M. Font-Bardía, *Inorg. Chem.* **1993**, *32*, 3727; d) R. Cortés, M. K. Urtiaga, L. Lezama, J. L. Pizarro, A. Goñi, M. I. Arriortua, T. Rojo, *Inorg. Chem.* **1994**, *33*, 4009; e) H.-Y. Shen, D.-Z. Liao, Z. -H. Jiang, S.-P. Yan, B.-W. Sun, G.-L. Wang, X.-K. Yao, H.-G. Wang, *Chem. Lett.* **1998**, 469; f) F. A. Mautner, S. Hanna, R. Cortés, M. G. Barandika, T. Rojo, *Inorg. Chem.* **1999**, *38*, 4647; g) C. S. Hong, S.-K. Son, Y. S. Lee, M.-J. Jun, Y. Do, *Inorg. Chem.* **1999**, *38*, 5602; h) M. A. M. Abu-Youssef, A. Escuer, D. Gatteschi, M. A. S. Goher, F. A. Mautner, R. Vincente, *Inorg. Chem.* **1999**, *38*, 5716.

[27] O. Kahn, *Molecular Magnetism*, VCH, New York, **1993**, p. 187.

[28] R. L. Carlin, *Magnetochemistry*, Springer, New York, **1986**, p. 14.

[29] a) J. M. Manriquez, J. P. Tuchagues, V. Petrouleas, J. M. Savariault, R. Poinsot, M. Drillon, *Inorg. Chem.* **1991**, *30*, 3587; b) E. Bakalbassis, P. Bergerat, O. Kahn, S. Jeannin, Y. Jeannin, Y. Dromzee, M. Guillot, *Inorg. Chem.* **1992**, *31*, 625.

[30] a) C. G. Barraclough, R. L. Martin, S. Mitra, *J. Chem. Phys.* **1970**, *53*, 1638; b) C. G. Barraclough, A. K. Gregson, S. Mitra, *J. Chem. Phys.* **1974**, *60*, 962; c) R. Mason, G. A. Williams, P. E. Fielding, *J. Chem. Soc. Dalton Trans.* **1979**, 676; d) S. Mitra, A. K. Gregson, W. E. Hatfield, R. R. Weller, *Inorg. Chem.* **1983**, *22*, 1729.

[31] J. Larionova, R. Clerac, J. Sanchiz, O. Kahn, S. Golhen, L. Ouahab, *J. Am. Chem. Soc.* **1998**, *120*, 13088.

[32] R. S. Drago, *Physical Methods for Chemists*, Saunders College, New York, **1992**.

[33] A. Altomare, G. Cascarano, C. Giacovazzo, A. Guagliardi, M. C. Burla, G. Polidor, M. J. Camallio, *J. Appl. Crystallogr.* **1994**, *27*, 435.

[34] G. M. Sheldrick, SHELXL-93, Program for Crystal Structure Refinement, Crystallographic Department, University of Göttingen (Germany), **1993**.

Received: May 7, 2001 [F3244]

  0947-6539/01/0719-4252 $ 17.50+.50/0 